ISSN 0036-0295, Russian Metallurgy (Metally), Vol. 2017, No. 7, pp. 579–584. © Pleiades Publishing, Ltd., 2017.
Original Russian Text © V.E. Kormyshev, V.E. Gromov, Yu.F. Ivanov, S.V. Konovalov, A.D. Teresov, 2017, published in Metally, 2017, No. 4, pp. 46–51.

# Structure and Properties of the Layer Deposited onto a Low-Carbon Steel and Then Irradiated by an Electron Beam

**V. E. Kormyshev[a, *], V. E. Gromov[a], Yu. F. Ivanov[b, c, **], S. V. Konovalov[a, d], and A. D. Teresov[b]**

[a] *Siberian State Industrial University, ul. Kirova 42, Novokuznetsk, 654007 Russia*
[b] *Institute of High Current Electronics, Siberian Branch, Russian Academy of Sciences, pr. Akademicheskii 2/3, Tomsk, 634021 Russia*
[c] *National Research Tomsk Polytechnic University, pr. Lenina 30, Tomsk, 634050 Russia*
[d] *Samara National Research University, Moskovskoe sh. 34, Samara, 443086 Russia*
**e-mail: ksv@ssau.ru*
***e-mail: yufi55@mail.ru*

Received July 29, 2016

**Abstract**—The phase composition and the mechanical and tribological properties of the layer that is deposited onto a martensitic low-carbon steel using a C–Cr–Nb–W flux cored wire and is additionally twice irradiated by a pulsed electron beam are studied by optical microscopy, scanning electron microscopy, transmission electron diffraction microscopy, X-ray diffraction analysis, wear resistance tests, and durometry. The wear resistance and the microhardness of the deposited layer increase manyfold with respect to the base material, and the friction coefficient of the layer decreases after electron-beam treatment. The increase in the mechanical and tribological properties of the deposited layer subjected to electron-beam treatment is shown to be due to the formation of a submicrocrystalline structure hardened by this treatment and due to the precipitation of the NbC niobium carbide.

*Keywords:* phase composition, structure, microhardness, facing, flux cored wire, electron-beam treatment

**DOI:** 10.1134/S0036029517070084

## INTRODUCTION

The studies in the field of deposition of composition coatings hardened by the particles consisting of carbides, borides, and other high-hardness and high-modulus phases have recently been quickened. Such coatings are effective under conditions of strong abrasive wear and impact loads and are applied in various industries. Their service properties are determined by the chemical and phase compositions of the coating material. To choose the materials that meet operating conditions, it is necessary to investigate their properties and structures in detail [1–5].

High-energy energy fluxes (plasma flows, powerful ion beams, laser beams, etc.) are often used as additional hardening surface treatment. High-energy electron beams are most effective among them [6–15].

The purpose of this work is to analyze the structure and the mechanical and tribological properties of a deposited layer modified by an high-energy pulsed electron beam.

## EXPERIMENTAL

As a base material, we used Hardox 450 steel having the following chemical composition (wt %): 0.19–0.26 C, 0.70 Si, 1.60 Mn, 0.25 Cr, 0.25 Ni, 0.25 Mo, 0.004 B, 0.025 P, 0.010 S, and Fe for balance.

Hardox 450 steel is characterized by a low alloying element content; therefore, it can easily be welded and machined. The fine-grained structure of the steel and its high hardness are achieved due to a special-purpose system of quenching steel sheets, which consists in rapid cooling of a rolled sheet without subsequent annealing. As a result, this steel effectively withstands most types of wear.

Facing was carried out with a PP-3 wire 1.6 mm in diameter; its chemical composition is (wt %) 1.3 C, 0.9 Mn, 1.1 Si, 7.0 Cr, 8.5 Nb, 1.4 W, and Fe for balance.

A layer was deposited onto the steel surface in the protective gas atmosphere consisting of 98 wt % Ar and 2 wt % $CO_2$ at a welding current of 250–300 A and an arc voltage of 30–35 V. The layer surface was irradiated by a high-energy electron beam in a SOLO

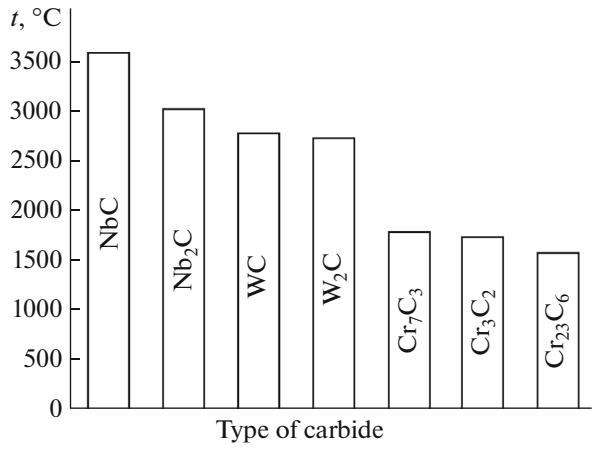


**Fig. 1.** Temperatures of the formation of the carbide phases based on niobium, tungsten, and chromium under equilibrium solidification conditions.

setup under melting and high-rate solidification conditions [14, 15]. The following operating conditions of the electron source were used for this purpose. At the first stage, the electron beam energy density per pulse was 30 J/cm$^2$, the pulse duration was 200 μs, and the number of pulses was 20. At the second stage, the electron beam energy density per pulse was 30 J/cm$^2$, the pulse duration was 50 μs, and the number of pulses was 1. The irradiation conditions were chosen on the basis of the results of calculating the temperature field formed in the surface layer of the material during one-pulse irradiation. Mechanical tests of the modified surface were carried out by determining the Vickers microhardness on a PMT-3 tester at a load of 0.2 and 0.5 N applied to an indenter and determining Young's modulus on a Shimadzu DUH-211S ultramicrohardness tester at a load of 50 mN applied to an indenter. Tribological tests of the modified surface were performed using a CSEM Tribometer High Temperature S/N 07-142 (CSEM Instruments, Switzerland) tribometer, and the wear rate was estimated from the cross-sectional area of a wear track using a MICRO MEASURE 3D (STIL, France) station. The structure of the material was examined by optical microscopy (μVizo-MET-221 metallographic microscope) and scanning electron microscopy (SEM-515 Philips microscope). The elemental composition of the surface layer was determined by electron-probe microanalysis with an EDAX ECON IV microanalyzer attached to the SEM-515 Philips scanning electron microscope. X-ray diffraction (XRD) with an XRD-7000s (Shimadzu, Japan) diffractometer was used to analyze the phase composition, the state of a crystal lattice, the microstresses, and the coherent domain size (CDS) in the surface layer.

## RESULTS AND DISCUSSION

Facing was found to result in the formation of a high-strength surface layer ~6 mm thick, and its average microhardness is ~10.2 GPa, which is higher than the microhardness of the base metal (Hardox 450 steel) by a factor of ~1.7. Irradiation of the deposited layer by a high-energy pulsed laser beam leads to an increase in the microhardness of the modified layer to ~13 GPa, which is higher than the microhardness of the initial steel by a factor of ~2.2. Simultaneously, Young's modulus (elastic modulus), which characterizes the ability of a material to withstand tension and compression during elastic deformation [16], increases by ~1.3 times.

The increase in the hardness of the deposited layer during the irradiation of its surface by an electron beam led to a multiple (by a factor of ~70) increase in its wear resistance during the friction of a ball made of a VK6 hard alloy on the surface of the deposited material. Here, the friction coefficient decreased by ~1.1 times.

Based on the composition of the wire used for facing, we can expect that the high tribological and strength properties of the deposited material are caused by hardening of the material by niobium, chromium, and tungsten carbides.

The Nb–C system is characterized by the presence of a niobium-based solid solution, the stable $Nb_2C$ and NbC phases, and the metastable $Nb_3C_2$ phase [17, 18]. An analysis of the available information demonstrates that the NbC carbide melts congruently at 46.2 at % C and a temperature of 3608 ± 50°C. The $Nb_2C$ carbide forms during the NbC → $Nb_2C$ resolidification at 2500°C. According to the data of most investigators, the $Nb_2C$ carbide forms according to the $L$ + NbC ⇄ $Nb_2C$ peritectic reaction at 34.5 at % C and a temperature of 3035 ± 20°C.

A comparative analysis of these results shows that the NbC niobium carbide has the maximum formation temperature (3608°C). Carbide β-$W_2C$ forms at a lower temperature (2785°C) and chromium carbide $Cr_7C_3$ forms at 1789°C (Fig. 1). Therefore, the main carbide during the solidification of the deposited layer is assumed to be niobium carbide NbC, the formation of which ensures high tribological and strength properties.

It should also be noted that both niobium and tungsten fix carbon and prevent the formation of chromium carbides in the steel and intercrystalline corrosion.

XRD studies of the phase composition of the deposited layer revealed the formation of NbC niobium carbide inclusions in the electron-beam-modified sublayer (see Fig. 2). The relative content of these inclusions is 53 wt % and the remaining content is represented by an α-iron-based solid solution. The NbC carbide has the maximum formation temperature

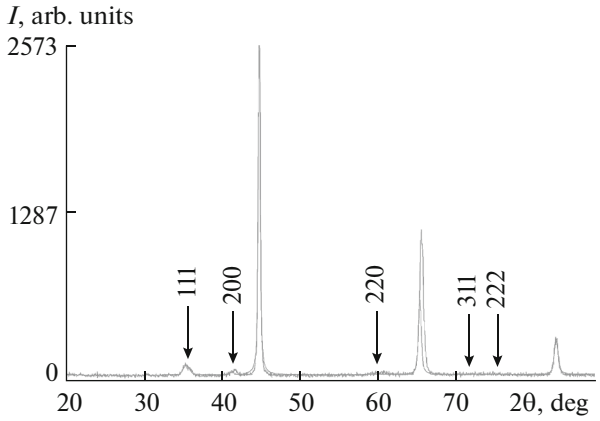


**Fig. 2.** X-ray diffraction pattern taken from the surface of the deposited layer additionally irradiated by an electron beam. The diffraction peaks of the niobium carbide are indicated.

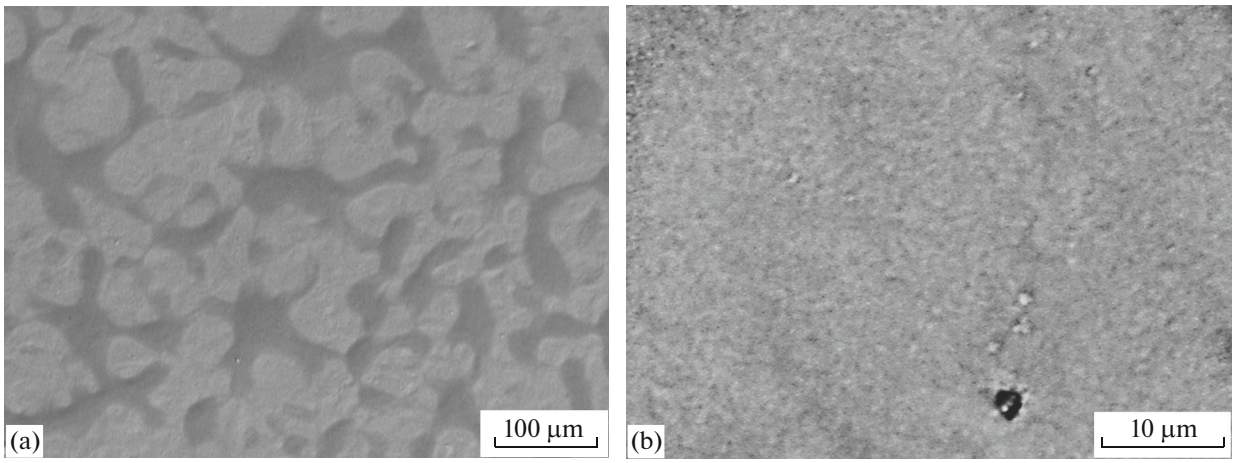


**Fig. 3.** SEM images of the surface structure of the deposited layer after irradiation by an electron beam.

among the carbides of the alloying elements in a PP-3 flux cored wire. The lattice parameter of the niobium carbide is $a = 0.43691$ nm. Since the lattice parameter of the NbC niobium carbide changes in the range 0.44317–0.44690 nm and increases with the carbon content under equilibrium conditions [17, 18], we assume that the niobium carbide that forms in the deposited layer during high-speed electron-beam treatment is depleted of carbon; that is, it is far from its equilibrium state. The CDS of the niobium carbide is $D_{CDS} = 12.69$ nm and the lattice microdistortion of the niobium carbide is $\Delta d/d = 6.47 \times 10^{-3}$.

Optical microscopy (OM) and scanning electron microscopy (SEM) studies revealed the formation of a eutectic structure in the surface layer, and its characteristic image is shown in Fig. 3a. The irradiation of the layer deposited onto the steel by a high-energy electron beam substantially refined the structure of the surface layer of the material (down to submicro- and nanosized states), which was caused ultrahigh cooling rates of the modified layer [14, 15]. The structural-element sizes change from 0.3 to 0.8 μm (Fig. 3b).

Figure 4 shows an OM image of the structure of a transverse polished section. The formed multilayer structure is seen to be represented by a 5-μm-thick surface layer (Fig. 4a, layer *1*) and an intermediate 20-μm-thick layer (layer *2*). When studying the structure of a transverse polished section, we were able to reveal the structure of the heat-affected zone (HAZ) that forms in the contact zone between the deposited layer and the Hardox 450 steel (see Fig. 4b). It was found that the deposition of a layer is accompanied by, first, a substantial increase in the grain size in HAZ in steel and, second, steel quenching (Fig. 5).

Figure 6 shows the structure of the deposited layer revealed by SEM upon studying the transverse polished section etched in the plasma of a low-pressure gas (argon) discharge. The electron-beam-modified layer was found to have a thickness of ~30 μm

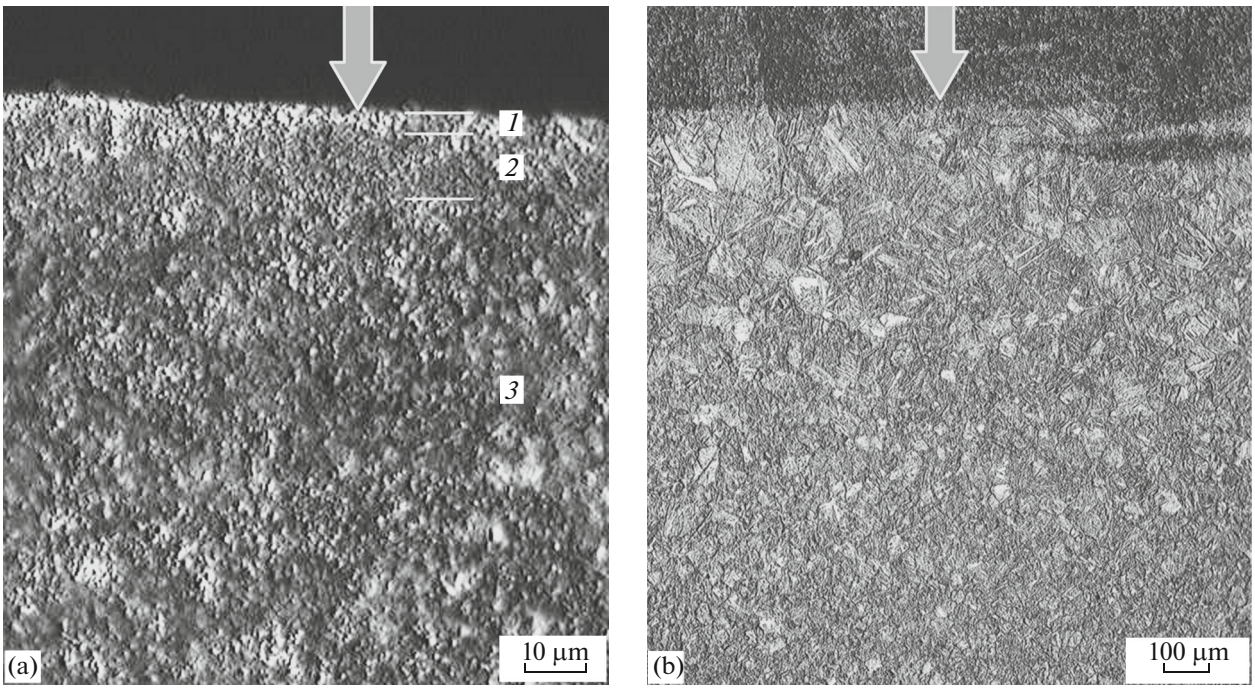


**Fig. 4.** OM images of the structure of a transverse polished section of the deposited layer after irradiation by an electron beam. The arrow in (a) indicates the modification surface, and the arrow in (b) indicates the layer separating the deposited metal and Hardox 450 steel.

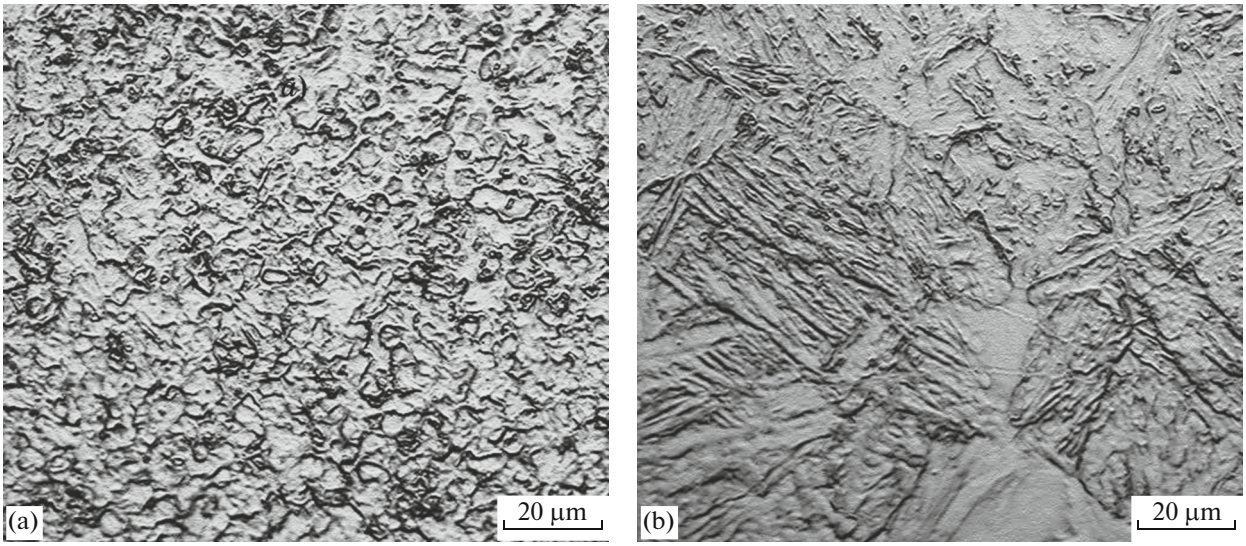


**Fig. 5.** Structure of the Hardox 450 steel formed (a) at a distance of 800 μm from the contact zone between the deposited layer and the base steel and (b) near the contact zone.

(Figs. 6a, 6b) and to be separated into two sublayers (Figs. 6b, 6c). Obviously, this separation is caused by the two-stage method of electron-beam irradiation of the surface of the deposited layer.

The irradiation of the deposited layer by a pulsed electron beam is accompanied by a substantial decrease in the structural-element size, which is due to the ultrahigh rates of solidification and subsequent cooling of the modified layer during pulsed electron-beam treatment of the material [14, 15]. An analysis of the images of a polished etched section presented in Figs. 6c and 6d demonstrates that the structural-element sizes in the modified layer change down to 0.5 μm (Fig. 6d) and the structural-element sizes in

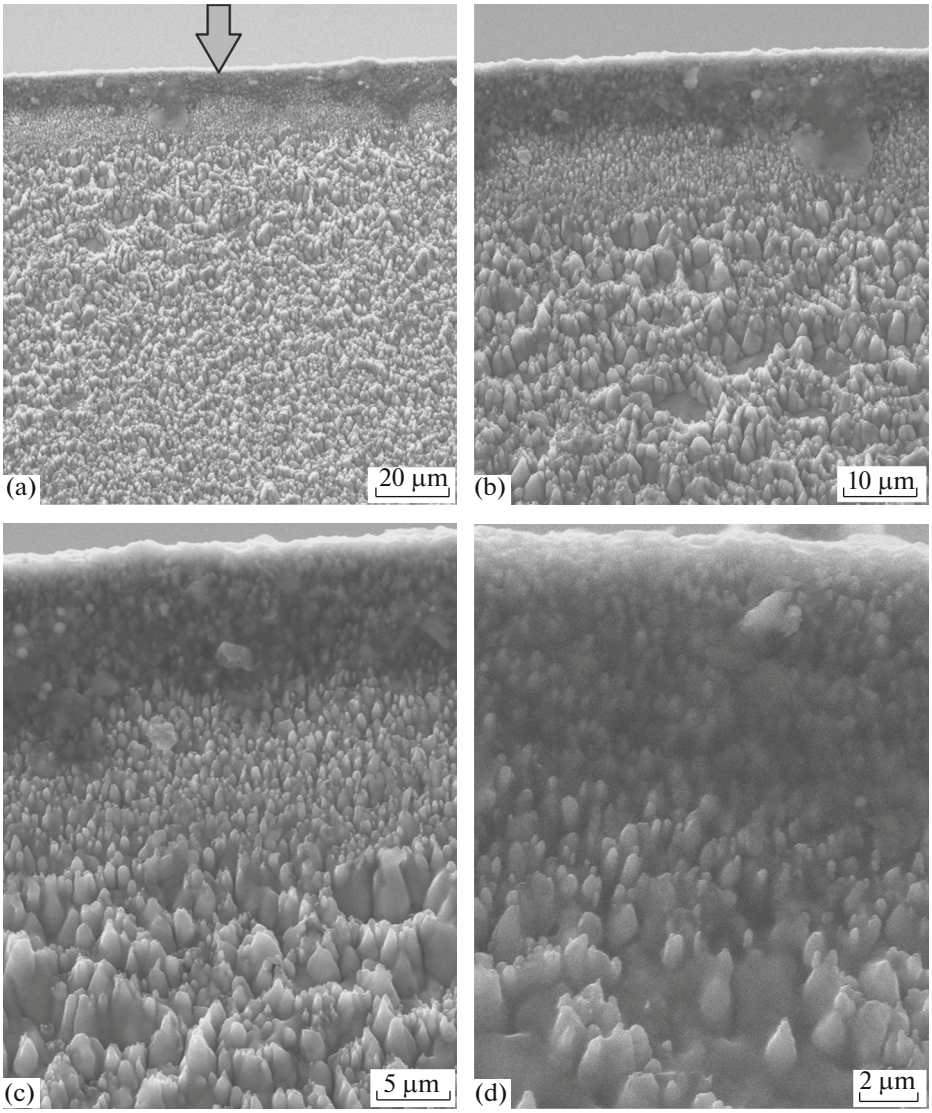


**Fig. 6.** SEM images of the structure of a transverse polished section of the deposited layer after electron-beam irradiation. The arrow in (a) indicates the modification surface. Etching was performed in the plasma of a low-pressure gas (argon) discharge.

the deposited layer under the modified layer decrease to 1 μm (Fig. 6c).

## CONCLUSIONS

(1) The phase composition, the defect substructure, and the mechanical and tribological properties of the layer that was deposited onto Hardox 450 steel during one passage of a flux cored wire and was additionally modified by the irradiation of a high-energy pulsed electron beam (two-stage method) were studied.

(2) The increase in the mechanical and tribological properties of the deposited layer modified by a pulsed electron beam was found to be due to the formation of a submicrocrystalline structure hardened because of ultrahigh heating and cooling rates and due to the precipitation of the NbC niobium carbide.

## ACKNOWLEDGMENTS

This work was supported by the Russian Science Foundation, project no. 15-19-00065.

## REFERENCES

1. I. M. Poletika, S. A. Makarov, M. V. Tetyutskaya, and T. A. Krylova, "Electron-beam deposition of wear-resistant and corrosion-resistant coatings onto a low-carbon steel," Izv. Tomsk. Polytekh. Univ. **321** (2), 86–89 (2012).
2. X. Qi, S. Zhu, H. Ding, Z. Zhu, and Z. Han, "Microstructure and wear behaviors of WC–12% Co coating deposited on ductile iron by electric contact surface strengthening," Appl. Surf. Sci. **282**, 672–679 (2013).
3. X. Chen, Y. Fang, P. Li, Z. Yu, X. Wu, and D. Li, "Microstructure, residual stress and mechanical prop-

erties of a high strength steel weld using low transformation temperature welding wires," Mater. Des. **65**, 1214–1221 (2015).

4. S. Konovalov, Y. Kormyshev, V. Gromov, and Yu. Ivanov, "Metallographic examination of forming improved mechanical properties via surfacing of steel HARDOX 450 with flux cored wire," Mater. Sci. Forum **870**, 159–162 (2016).
5. S. V. Konovalov, V. E. Kormyshev, V. E. Gromov, Yu. F. Ivanov, and E. V. Kapralov, "Phase composition and defect substructure of the binary facing formed by a C–V–Cr–Nb–W flux cored wire on Hardox 450 steel," Perspekt. Mater., No. 8, 57–63 (2016).
6. J. C. Walker, J. W. Murray, M. Niea, R. B. Cook, and A. T. Clare, "The effect of large-area pulsed electron beam melting on the corrosion and microstructure of a Ti6A14V alloy," Appl. Surf. Sci. **311**, 534–540 (2014).
7. Yu-Kui Gao, "Influence of pulsed electron beam treatment on microstructure and properties of TA15 titanium alloy," Appl. Surf. Sci. **264**, 633–635 (2013).
8. Guodong Zhang, Xinqi Yang, Xinlong He, Jinwei Li, and Haichao Hu, "Enhancement of mechanical properties and failure mechanism of electron beam welded 300M ultrahigh strength steel joints," Mater. Des. **45**, 56–66 (2013).
9. M. G. Golkovski, I. A. Bataev, A. A. Bataev, A. A. Ruktuev, T. Y. Zhuravina, N. K. Kuksanov, R. A. Salimov, and V. A. Bataev, "Atmospheric electron-beam surface alloying of titanium with tantalum," Mater. Sci. Eng. A **578**, 310 (2013).
10. J. C. Oh, E. Yun, M. G. Golkovski, and S. Lee, "Improvement of hardness and wear resistance in SiC/Ti–6Al–4V surface composites fabricated by high-energy electron beam irradiation," Mater. Sci. Eng. A **351** (1–2), 98–108 (2003).
11. X. D. Zhang, J. X. Zou, S. Weber, S. Z. Hao, C. Dong, and T. Grosdidier, "Microstructure and property modifications in a near α-Ti alloy induced by pulsed electron beam surface treatment," Surf. Coat. Technol. **206**, 295–304 (2011).
12. V. A. Gribkov, F. I. Grigor'ev, B. A. Kalin, et al., *Promising Radiation-Beam Technologies of Material Treatment: Tutorial* (Kruglyi Stol, Moscow, 2001).
13. K. K. Kadyrzhanov, F. F. Komarov, A. D. Pogrebhyak, et al., *Ion-Beam and Ion-Plasma Modification of Materials* (Izd. MGU, Moscow, 2005).
14. V. Rotshtein, Yu. Ivanov, and A. Markov, "Surface treatment of materials with low-energy, high-current electron beams," in *Materials Surface Processing by Directed Energy Techniques*, Ed. by Y. Pauleau (Elsevier, 2006), Ch. 6, pp. 205–240.
15. V. E. Gromov, Yu. F. Ivanov, S. V. Vorobiev, and S. V. Konovalov, *Fatigue of Steels Modified by High Intensity Electron Beams* (Cambridge Intern. Sci. Publ., Cambridge, 2015).
16. A. P. Babichev, N. A. Babushkina, A. M. Bratkovskii, et al., *Physical Quantities: A Handbook* (Energoatomizdat, Moscow, 1991).
17. O. A. Bannykh, P. B. Budberg, S. P. Alisova, et al., *Binary and Multicomponent Iron-Based Alloy Phase Diagrams* (Metallurgiya, Moscow, 1986).
18. *Phase Diagrams of Binary Metallic Systems: A Handbook*, Ed. by N. P. Lyakishev (Mashinostroenie, Moscow, 1996), Vol. 1.

*Translated by K. Shakhlevich*